From operculum and body tail movements to different coupling of physical activity and respiratory frequency in farmed gilthead sea bream and European sea bass. Insights on aquaculture biosensing

Miguel A. Ferrer[a], Josep A. Calduch-Giner[b], Moises Díaz[a,c], Javier Sosa[d], Enrique Rosell-Moll[b] Judith Santana Abril[d], Graciela Santana Sosa[d], Tomás Bautista Delgado[d], Cristina Carmona[a], Juan Antonio Martos-Sitcha[b,e], Enric Cabruja[f], Juan Manuel Afonso[g], Aurelio Vega[d], Manuel Lozano[f], Juan Antonio Montiel-Nelson[d], Jaume Pérez-Sánchez[b,*]

[a]Technological Centre for Innovation in Communications (iDeTIC), University of Las Palmas de Gran Canaria, Las Palmas, Spain

[b]Nutrigenomics and Fish Growth Endocrinology Group, Institute of Aquaculture Torre de la Sal, Consejo Superior de Investigaciones Científicas (CSIC), Castellón, Spain

[c]Universidad del Atlántico Medio, Las Palmas, Spain

[d]Institute for Applied Microelectronics (IUMA), University of Las Palmas de Gran Canaria, Las Palmas, Spain

[e]Department of Biology, Faculty of Marine and Environmental Sciences, Instituto Universitario de Investigación Marina (INMAR), Campus de Excelencia Internacional del Mar (CEI-MAR), University of Cádiz, 11519 Puerto Real, Cádiz, Spain.

[f]Institute of Microelectronics of Barcelona (IMB-CNM), Consejo Superior de Investigaciones Científicas (CSIC), Barcelona, Spain

[g]Aquaculture Research Group, Institute of Sustainable Aquaculture and Marine Ecosystems (IU-ECOAQUA), University of Las Palmas de Gran Canaria, Las Palmas, Spain.

*Corresponding author:

Jaume Pérez-Sánchez

jaime.perez.sanchez@csic.es

Highlights:

- AEFishBIT provides simultaneous measures of fish respiration and locomotion.
- Device measures highlight species differences in anatomical and locomotor features.
- Coupling of activity and respiration rhythms emerges as fish performance indicator.

Abstract

The AEFishBIT tri-axial accelerometer was externally attached to the operculum to assess the divergent activity and respiratory patterns of two marine farmed fish, the gilthead sea bream (*Sparus aurata*) and European sea bass (*Dicentrarchus labrax*). Analysis of raw data from exercised fish highlighted the large amplitude of operculum aperture and body tail movements in European sea bass, which were overall more stable at low-medium exercise intensity levels. Cosinor analysis in free-swimming fish (on-board data processing) highlighted a pronounced daily rhythmicity of locomotor activity and respiratory frequency in both gilthead sea bream and European sea bass. Acrophases of activity and respiration were coupled in gilthead sea bream, acting feeding time (once daily at 11:00 h) as a main synchronizing factor. By contrast, locomotor activity and respiratory frequency were out of phase in European sea bass with activity acrophase on early morning and respiration acrophase on the afternoon. The daily range of activity and respiration variation was also higher in European sea bass, probably as part of the adaptation of this fish species to act as a fast swimming predator. In any case, lower locomotor activity and enhanced respiration were associated with larger body weight in both fish species. This agrees with the notion that selection for fast growth in farming conditions is accompanied by a lower activity

profile, which may favor an efficient feed conversion for growth purposes. Therefore, the use of behavioral monitoring is becoming a reliable and large-scale promising tool for selecting more efficient farmed fish, allowing researchers and farmers to establish stricter criteria of welfare for more sustainable and ethical fish production.

Keywords (**max. 6**): fish, accelerometers, physical activity, respiratory frequency, energy partitioning, welfare and selective breeding.

1. Introduction

Accelerometers are widely used to assess physical activity in public health (Vale et al., 2015) as they provide reliable measurements of energy expenditure and time spent in different activity conditions (Crouter et al., 2018). Certainly, activity recognition by means of specific algorithms allows the risk assessment of sedentary lifestyle and overweight in aged people (Taylor et al., 2014) and children (Duncan et al., 2016; Roscoe et al., 2019), which enables the use of accelerometer records for extracting quantitative measures of biological age (Pyrkov et al., 2018). Since the late 1990s, researchers have also employed portable accelerometers to investigate energy expenditure, activity patterns and the postural behavior of livestock, companion animals, free-ranging species, laboratory animals and zoo-housed species (Brown et al., 2013; Whitham and Miller, 2016). However, it is important to certify that these devices do not negatively impact the animals and, hence, skew the data. Thus, important research efforts are focused on how and where the device is attached. Common attachment methods include collars, anklets, harnesses and clamps, and the placement of the device determines the type of behavior that can be monitored (Brown et al., 2013). Furthermore, to consider whether the subject or conspecifics can remove the device is a key factor (Rothwell et al., 2011), and whether color, mass or shape affect the animal behavior, limiting the functional value of the registered data is also of importance (Wilson et al., 2008). Ruminants are, however, a case of high success and a number of studies clearly indicate that feeding behavior (Alvarenga et al., 2016; Rayas-Amor et al., 2017), rumen mobility (Michie et al., 2017; Hamilton et al., 2019) or positive affective states affecting diseases and other welfare concerns (de Oliveira and Keeling, 2018) are measurable by accelerometers, contributing to improve animal welfare and productivity.

Like in terrestrial livestock, the biosensor technology has the potential to revolutionize the aquaculture industry (Andrewartha et al., 2016; Endo and Wu, 2019; Rajee and Alicia, 2019), but the state-of-the-art of micro-systems provide limited real-time access to telemetry data (Føre et al., 2018; Hassan et al., 2019). Size and energy autonomy are also obvious limitations, and the choice of tagging method (external, attachment, surgical implantation), operational mode (stand-alone *vs.* wireless systems) and telemetry technology (*e.g.* radio-transmitters, acoustic transmitters, pop-up satellite archival tags) ultimately depends on life species, life stage and research question (Thorstad et al., 2013; Jepsen et al., 2015). Thus, small and light devices working in stand-alone mode appear especially suitable for quickly tracking challenged fish at specific time windows, allowing farmers and breeders to orientate selective breeding towards more robust and efficient fish or improve culture conditions for a more sustainable and ethical production. These are the criteria used within the AQUAEXCEL^{2020} EU project for the design of AEFishBIT, a patented (P201830305), stand-alone, small and light (1 g) motion embedded-microsystem based in a tri-axial accelerometer that is externally attached to the operculum to monitor physical activity by mapping accelerations in x- and y-axes, while operculum beats (z-axis) serve as a measurement of respiratory frequency (Martos-Sitcha et al., 2019). The accuracy of on-board algorithms was calibrated in swim metabolic chambers, and accelerometer outputs of exercised gilthead sea bream (*Sparus aurata*) and European sea bass (*Dicentrarchus labrax*) juveniles correlated with data on swimming speed and oxygen consumption. However, these two economically important marine farmed fish exhibit different locomotor capabilities, and we aimed to provide new insights into their divergent patterns of activity and energy partitioning between growth and locomotor activities. To pursue this global aim, raw data from forced exercised fish in metabolic chambers (15 min)

were retrieved to analyze the frequency and amplitude of operculum and body tail movements. Additionally, new post-processed data using on-board algorithms were obtained over extended recording periods (2 days) to assess the behavioral patterns of free-swimming fish in rearing tanks. Such approach reinforced the different adaptive strategies of gilthead sea bream and European sea bass that primarily arise from changes in body shape and specialized movements, but also from the different coupling on a daily basis of physical activity and respiratory frequency.

2. Materials and methods

2.1. Swim tunnel and raw data download

Data from exercised juveniles of gilthead sea bream (n=18) and European sea bass (n=15) in a swim tunnel respirometer (Loligo® Systems, Viborg, Denmark) were retrieved from Martos-Sitcha et al. (2019) for raw data analyses. Briefly, fish were exercised at three increasing speeds (1, 2 and 3 BL/s) lasting 5 min each consecutive period. Accelerometers were programmed for the acquisition of data sets for 2 min at each swimming speed at a sampling period of 100 *Hz*. After testing, fish were removed from the tunnel and the device was plugged-out for data downloading and raw data off-line post-processing.

2.2. Raw data processing

The signal from the z-axis, that records the operculum opening and closing, was numerically integrated to assess the velocity of the operculum movement. This integration

minimized the influence of other movements such as lateral body movements or angular velocity:

$$v_{zr}(t) = \int_0^t a_z(t)dt$$

To remove the trend of $v_{zr}(t)$, it was high pass filtered by a filter cut-off frequency of $f_c = 1\ Hz$ that allows breathing frequency pass through. The high pass filter was carried out in two steps: a) $v_{zr}(t)$ was low pass filtered by 1 Hz cut-off filter obtaining $v_{zlp}(t)$, and b) the detrended velocity of the operculum was estimated as $v_z(t) = v_{zr}(t) - v_{zlp}(t)$. The distance run by the operculum can be approached by integrating $v_z(t)$. Details and examples of processed signals and raw data are provided as **Supplemental file S1**.

Operculum opening can be defined as the distance increase from zero to maximum aperture, as illustrated in the synthetic example of **Figure 1A**. The velocity was zero at the beginning and at the end of the opening, so the velocity increased and decreased in a bell-shaped way, as exemplified in **Figure 1B**. In consequence, the acceleration (**Figure 1C**) started high and positive during the first phase of the operculum opening and decreased to negative values, whereas the operculum started to stop at the second phase of the operculum opening.

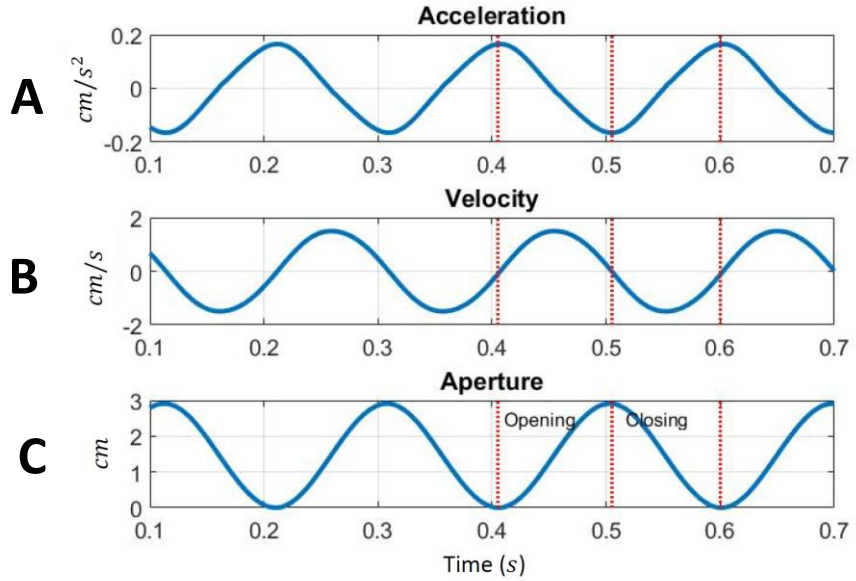

Figure 1. Synthetic example of aperture distance, velocity and acceleration during operculum movement. Acceleration is the derivate of the velocity and velocity the derivate of distance. **A.** Operculum closing (aperture = 0) and opening (maximum aperture) along time. **B.** Operculum velocity. **C.** Operculum acceleration. During operculum opening, velocity is positive and acceleration goes from positive to negative. During operculum closing closing, velocity is negative and acceleration goes from negative to positive.

Figure 1 is consistent with the kinematic theory of the rapid movement that establishes a lognormality principle, which allows modelling the output velocity of a complex neuromuscular system through an overlapped sequence of lognormal functions. Based on the application of this principle, rapid human hand movements have been modeled (Plamondon et al., 2014; Diaz et al., 2015; Duval et al., 2015), and the same approach was used herein for modelling the operculum movement. After that, elemental opening and closing movements are represented as the following sequence of lognormal-shape velocity profiles (or lognormals):

158 $$v(t) = \sum_i v_i\left(t; t_{o_i}, \mu_i, \sigma_i^2\right)$$

159 Being each velocity profile

160 $$v_i\left(t; t_{o_i}, \mu_i, \sigma_i^2\right) = \frac{\mathrm{D}_i}{\sigma_i\sqrt{2\pi}(t - t_{o_i})} \exp\left(-\frac{\left[\ln\left(t - t_{o_i}\right) - \mu_i\right]^2}{2\sigma_i^2}\right)$$

161 where t is time; t_{oi}, time of movement occurrence; D_i, area of the velocity; μ_i, time delay;
162 σ_i, response time of each lognormal of the sequence. Both μ_i and σ_i are expressed on a
163 logarithmic time scale. Thus, basic movements (opening or closing) of the operculum can
164 be parameterized with t_{oi}, D_i, μ_i and σ_i as exemplified in **Figure 2**.

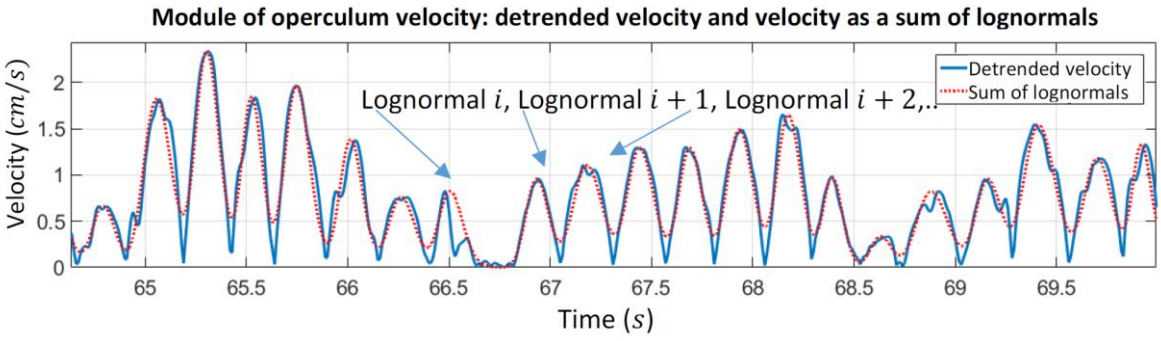

165

166 **Figure 2. Module of the detrended velocity decomposed as a sum of lognormals.**

167

168 Data measurements of operculum velocity yielded other parameters derived from
169 the lognormal function:

170 1. D or area of the lognormal (distance run by the lognormal).
171 2. μ or lognormal time delay.
172 3. σ or lognormal response time.

173

Additional parameters were obtained from the lognormal shape (**Figure 3**):

4. Temporal width (s): $t_3 - t_1$, time interval of a single movement.
5. Rise time (s): $t_2 - t_1$, time span of positive acceleration (velocity increment).
6. Drop time (s): $t_3 - t_2$, time span of negative acceleration (velocity decrement).
7. Lognormal skew, which estimates the velocity shape asymmetry. A skewness value between -0.5 and 0.5 means a fairly symmetrical movement. A skewness value > 0.5 indicates that the first phase of the movement is quicker than the second.
8. Kurtosis of the lognormal to estimate the "tailedness" of the velocity shape. A value of 3 means a Gaussian shape. Values larger than 3 indicate a leptokurtic movement, with extended tails and sharper and higher peaks.

The values of these eight parameters were obtained using iDeLog software, which includes recent improvements in the Sigma-Lognormal model (Ferrer et al., 2018).

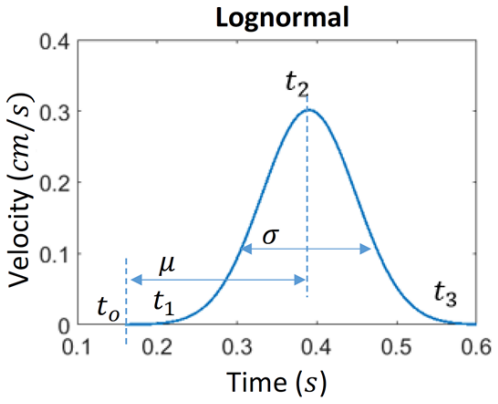

Figure 3. Temporal markers of operculum velocity lognormal. t_1 and t_3 are the times in which the lognormal value was the 5% of its maximum value. t_2 is the time in which the lognormal value was maximum (mode).

A similar procedure was conducted to model the velocity of the x- and y-axis, which defined the body tail movement. First, the accelerometer signals for both axes were numerically integrated:

$$v_{xr}(t) = \int_0^t a_x(t)dt$$

$$v_{yr}(t) = \int_0^t a_y(t)dt$$

Such velocities were detrended with a similar procedure than above obtaining $v_x(t)$ and $v_y(t)$. Then, the velocity of the body tail movement was estimated as $v_b(t) = \sqrt{v_x^2(t) + v_y^2(t)}$. This velocity was decomposed in a family of lognormals functions, which allows the extraction of the eight parameters mentioned above.

2.3. Free-swimming monitoring by means of on-board algorithms

To assess the free-swimming activity patterns of cultured fish, AEFishBIT measures were obtained from 3-year old gilthead sea bream (917.0 ± 37.2 g, n=8) and European sea bass (645.1 ± 49.3 g body weight, n=8) reared in 3,000 L tanks (8-10 kg/m^3) at the indoor experimental facilities of Institute of Aquaculture Torre de la Sal (IATS-CSIC) under natural photoperiod and temperature conditions (40º 5'N; 0º 10'E). Fish were fed once daily at 11:00 h, being overnight fasted the day of device tagging. The devices used for data recording were adequately packaged in silicone for water protection (14 x 7 x 7 mm), with a resulting weight in air of 1.1 g. The devices were externally attached to the operculum using metal Monel piercing fish tags (National Band & Tag Company, Newport, KY, United States) with a flexible heat shrink polyethylene tube (Eventronic, Shenzen, China)

212 that is able to easily fit the device as shown at https://vimeo.com/325943543. In skilled
213 hands, the entire application procedure took less than 30 s per fish and no pathological
214 signs of hemorrhage or tissue damage were found after 2-3 weeks of device tagging.
215 Devices were programmed for on-board calculation of respiratory frequency and physical
216 activity over 2 min time windows each 15 min along two consecutive days. Fish remained
217 unfed over the recording time, and the devices were retrieved for downloading the
218 processed data just after data recording was completed. For each device, clock time drift
219 was previously estimated for post-processing synchronization. This time drift was
220 established to be constant for a given device in a temperature range of 4-30 ºC.
221

222 2.4. Statistical analysis

223 Interspecies comparisons for raw data results derived from operculum and body tail
224 movements was conducted through the non-parametric Mann-Whithney U-test, using the
225 Matlab statistical toolbox. Analysis of on-board processed data of physical activity and
226 respiratory frequency was assessed through Student's t-test and Pearson coefficients using
227 the Sigmaplot suite (Systat Software Inc., Chicago USA). The daily rhythmicity of this
228 time series analysis was further analyzed using a simple cosinor model (Refinetti et al.,
229 2007).
230

231 2.5 Ethics statement

232 No mortalities were observed during fish manipulation and experimental procedures. All
233 procedures described herein were approved by the Ethics and Animal Welfare Committee

of IATS-CSIC and carried out according to the National (Royal Decree RD53/2013) and the current EU legislation (2010/63/EU) on the handling of experimental fish.

3. Results

3.1. Outlook of operculum movements

Lognormals derived from z-axis signal were aligned by fixing $t_0 = 0$. For each species and swim speed, the average shape of alternate velocity lognormals (i.e. shape comparison of operculum opening and closing movements) was the same (**Supplemental Figure S1**), and both movements were considered as equivalent for calculations. Averaged lognormals are summarized in **Table 1**. For a given speed, the averaged values of temporal widths (t3 - t1, time for operculum opening or closing) were consistently lower in gilthead sea bream than European sea bass. In both species, rise time (t2 - t1, related with the agonist's muscle of the movement) was lower than drop time (t3 - t2, related with the antagonist's muscle) at any swim speed, indicating that the agonist muscle of the movement was always quicker than the antagonist one. Positive values of skewness confirmed this fact, as it indicated that the velocity profile was skewed towards left with a tail on the right side. Regarding the area of the lognormal (aperture of the operculum), D, it was always larger in European sea bass than in gilthead sea bream at any given velocity, indicating a greater operculum aperture in European sea bass. Overall, these parameters pointed out that this species breathes fewer times per second than gilthead sea bream, also showing a larger aperture of the operculum with a higher ability to keep a stable movement with changes in swim speed.

Table 1. Parameters of operculum velocity averaged lognormal for exercised gilthead sea bream and European sea bass. Values are the mean ± SD of the device for 2 minutes raw data measures from operculum movements of 18 gilthead sea bream individuals and 15 European sea bass individuals. For a given fish species and parameter, different superscript letters reflect significant ($P < 0.001$) differences with swimming speed. For a given swimming speed and parameter, asterisk reflects significant ($P < 0.001$) differences between fish species. For a given fish species and swimming speed, italics in $t_2 - t_1$ reflect significant ($P < 0.001$) differences with the corresponding $t_3 - t_2$.

	Gilthead sea bream			European sea bass		
	1 BL/s	2 BL/s	3 BL/s	1 BL/s	2 BL/s	3 BL/s
$t_3 - t_1$	0.345±0.102^{a,*}	0.257±0.095^{b,*}	0.183±0.067^{c,*}	0.390±0.096^{a}	0.302±0,093^{b}	0.208±0.067^{c}
$t_2 - t_1$	*0.146±0.036*^{a,*}	*0.112±0.035*^{b,*}	*0.083±0.026*^{c,*}	*0.163±0.034*^{a}	*0.130±0.035*^{b}	*0.093±0.027*^{c}
$t_3 - t_2$	0.199±0.067^{a,*}	0.145±0.060^{b,*}	0.100±0.041^{c,*}	0.227±0.062^{a}	0.172±0.058^{b}	0.115±0.041^{c}
Skew	0.280±0.065^{a,*}	0.221±0.065^{b,*}	0.167±0.049^{c,*}	0.309±0.062^{a}	0.251±0.063^{b}	0.186±0.049^{c}
Kurt	3.147±0.079^{a,*}	3.094±0.067^{b,*}	3.054±0.041^{c,*}	3.177±0.073^{a}	3.120±0.062^{b}	3.066±0.039^{c}
μ	-0.476±0.050^{a,*}	-0.526±0.048^{b,*}	-0.571±0.035^{c,*}	-0.453±0.049^{a}	-0.500±0.052^{b}	-0.555±0.039^{c}
σ	0.093±0.021^{a,*}	0.073±0.021^{b,*}	0.056±0.016^{c,*}	0.102±0.020^{a}	0.083±0.021^{b}	0.062±0.016^{c}
D	0.245±0.002^{a,*}	0.290±0.002^{b,*}	0.313±0.002^{c,*}	0.351±0.002^{a}	0.363±0.002^{b}	0.434±0.004^{c}

With the increase of swimming speed, temporal width decreased in both species, with a concomitant decrease of rise and drop times, as well as σ and kurtosis. This increase of the respiratory frequency with increasing swimming speed was accompanied by an

increase of D and a lowering of skewness, so the velocity profiles became more symmetric (**Figure 4**). These findings were indicative of an increase of the respiratory frequency and a larger operculum opening with increasing swimming speed in both species.

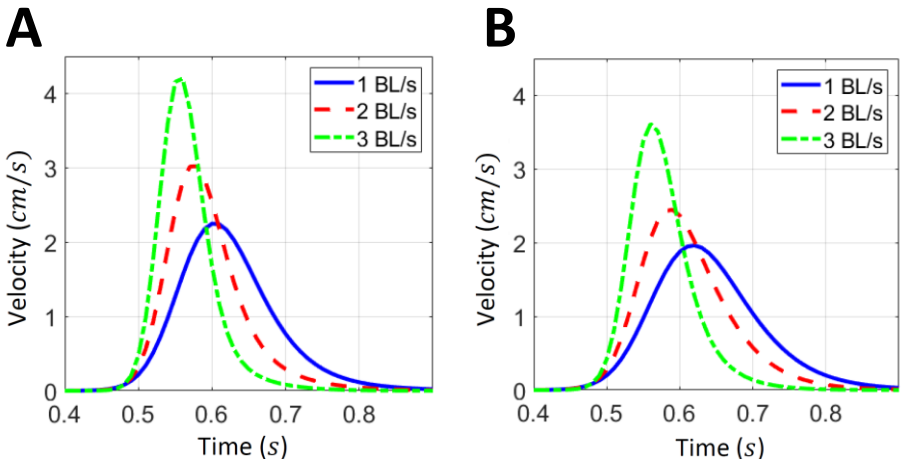

Figure 4. Average velocity lognormals of operculum movement. A. gilthead sea bream. **B.** European sea bass. Lognormals are represented at 1 BL/s (continuous blue), 2 BL/s (discontinuous red) and 3 BL/s (discontinuous green).

3.2. Outlook of body tail movements

Similarly to operculum movement analysis, all lognormals were aligned by fixing $t_0 = 0$. Averaged lognormals of gilthead sea bream and European sea bass body tail movements at different swimming speeds are summarized in **Table 2**. With the increase of water speed, temporal width decreased in both species, but it was sharper in t_3 - t_2 than in t_2 - t_1, which again suggests that the antagonist muscle become more and more active as swimming speed increases. It was also noticeable that D increased with swim speed in the case of gilthead sea bream, but it remained quite unaltered in European sea bass. This would imply that in order to compensate the increasing speed, European sea bass would increase the

frequency of the movement, while gilthead sea bream would need to increase both frequency and amplitude of the body tail movement.

Table 2. Values of body movement velocity averaged lognormal for exercised gilthead sea bream and European sea bass. Values are the mean ± SD of the device for 2 minutes raw data measures from body tail movements of 18 gilthead sea bream individuals and 15 European sea bass individuals. For a given fish species and parameter, different superscript letters reflect significant ($P < 0.001$) differences with swimming speed. For a given swimming speed and parameter, asterisk reflects significant ($P < 0.001$) differences between fish species. For a given fish species and swimming speed, italics in $t_2 - t_1$ reflect significant ($P < 0.001$) differences with the corresponding $t_3 - t_2$.

	Gilthead sea bream			European sea bass		
	1 BL/s	2 BL/s	3 BL/s	1 BL/s	2 BL/s	3 BL/s
$t_3 - t_1$	0.387±0.135^{a,*}	0.290±0.105^{b,*}	0.209±0.083^{c,*}	0.416±0.126^{a}	0.309±0.090^{b}	0.231±0.073^{c}
$t_2 - t_1$	*0.160±0.046*^{a,*}	*0.125±0.039*^{b,*}	*0.093±0.033*^{c,*}	*0.171±0.043*^{a}	*0.132±0.036*^{b}	*0.102±0.029*^{c}
$t_3 - t_2$	0.227±0.089^{a,*}	0.166±0.066^{b,*}	0.116±0.050^{c,*}	0.245±0.083^{a}	0.177±0.062^{b}	0.129±0.045^{c}
Skew	0.310±0.090^{a,*}	0.247±0.076^{b,*}	0.188±0.063^{c,*}	0.329±0.083^{a}	0.261±0.070^{b}	0.205±0.056^{c}
Kurt	3.186±0.113^{a,*}	3.119±0.078^{b,*}	3.070±0.051^{c,*}	3.206±0.105^{a}	3.130±0.072^{b}	3.080±0.046^{c}
μ	-0.473±0.059^{a,*}	-0.520±0.049^{b,*}	-0.561±0.039^{c,*}	-0.459±0.058^{a}	-0.512±0.048^{b}	-0.552±0.039^{c}
σ	0.103±0.029^{a,*}	0.082±0.025^{b,*}	0.062±0.021^{c,*}	0.109±0.027^{a}	0.086±0.023^{b}	0.068±0.018^{c}
D	0.263±0.003^{a,*}	0.334±0.003^{b,*}	0.362±0.003^{c,*}	0.252±0.003^{a}	0.214±0.003^{b}	0.259±0.004^{a}

3.3. Free-swimming temporal patterns of physical activity and respiration

Recorded data from incomplete light and dark phases, corresponding to the beginning and the end of the experimental period, were excluded to avoid any temporal bias. Thus, the analyzed period for all implanted individuals comprised two complete dark and one complete light phase. Mean values over time were extracted for preliminary analysis (**Supplemental Figure S2**), and they were quite similar to the calculated mesor by means of cosinor analysis. For a given species, mesor values remained fairly constant among individuals, but pronounced differences were found between gilthead sea bream and European sea bass. Hence, the retrieved physical activity of gilthead sea bream was significantly higher than that of European sea bass (0.080 ± 0.006 *vs.* 0.057 ± 0.002, $P < 0.01$). Conversely, respiratory frequency was significantly lower in European sea bass (1.57 ± 0.04 *vs.* 1.73 ± 0.04, $P < 0.05$). In both fish species, correlation analysis of individual body weight with their own physical activity and respiratory frequency resulted in negative and positive correlations, respectively (**Table 3**). This stated that, for a given species, larger fish showed a lower physical activity and a higher respiratory frequency than their smaller congeners of the same age.

Table 3. Pearson correlation coefficients between individual body weight and physical activity and respiratory frequency indexes in gilthead sea bream and European sea bass. P-value obtained in Pearson correlation is indicated in parentheses.

	Gilthead sea bream	European sea bass
Physical activity index	-0.717 (0.109)	-0.447 (0.050)
Respiratory frequency	0.811 (0.267)	0.613 (0.106)

Cosinor analysis of AEFishBIT recorded data showed clear daily rhythmic variations (**Figure 5**). For both fish species, the acrophase (time of peak value) of physical activity occurred few hours after the light onset, acting the pre-existing feeding time at 11:00 h as a main synchronizing factor (**Figure 5A, 5D**). In gilthead sea bream, a high level of synchronicity between physical activity index (**Figure 5A**) and respiratory frequency (**Figure 5B**) was found, as evidenced by the positive correlation of extracted data (**Figure 5C**). By contrast, European sea bass exhibited quite different activity patterns for physical activity index (**Figure 5D**) and respiratory frequency (**Figure 5E),** which showed a maximum value on the afternoon (acrophase at 18:04 h). This yielded an overall negative correlation between physical activity and respiration during almost all the recording time (**Figure 5F).** Dynamics of recorded parameters also highlighted species-specific differences on the amplitude of the adjusted curves, which were 1.5- (physical activity) or 2-fold (respiratory frequency) higher in European sea bass than in gilthead sea bream.

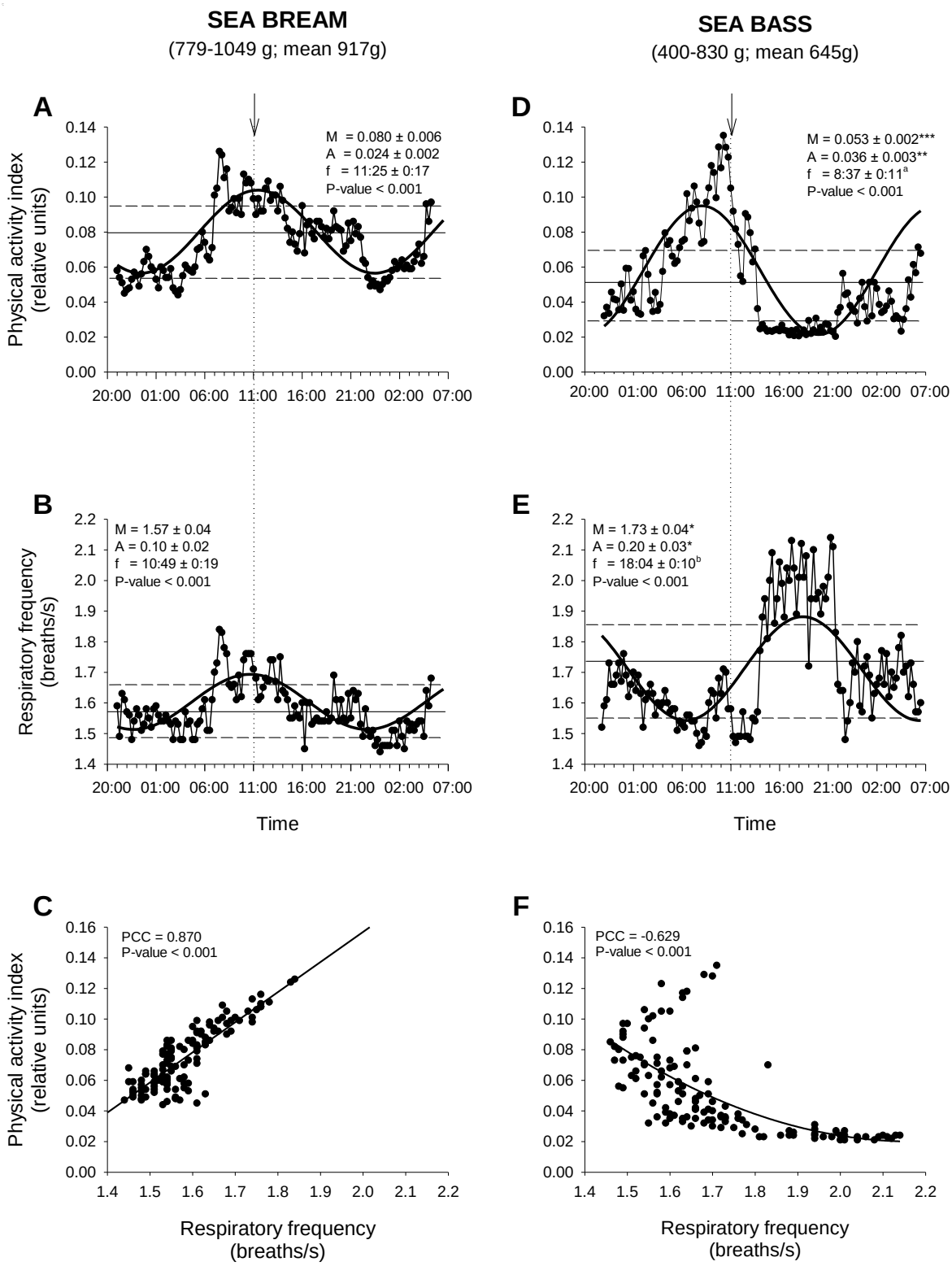
SEA BREAM
(779-1049 g; mean 917g)
SEA BASS
(400-830 g; mean 645g)
A
M = 0.080 ± 0.006
A = 0.024 ± 0.002
f = 11:25 ± 0:17
P-value < 0.001
D
M = 0.053 ± 0.002***
A = 0.036 ± 0.003**
f = 8:37 ± 0:11a
P-value < 0.001
Physical activity index (relative units)
B
M = 1.57 ± 0.04
A = 0.10 ± 0.02
f = 10:49 ± 0:19
P-value < 0.001
E
M = 1.73 ± 0.04*
A = 0.20 ± 0.03*
f = 18:04 ± 0:10b
P-value < 0.001
Respiratory frequency (breaths/s)
20:00 01:00 06:00 11:00 16:00 21:00 02:00 07:00
Time
C
PCC = 0.870
P-value < 0.001
F
PCC = -0.629
P-value < 0.001
Physical activity index (relative units)
Respiratory frequency (breaths/s)

334
335

Figure 5. Consensus activity patterns from AEFishBIT measures. Daily variation of physical activity index (**A**, sea bream; **D**, sea bass) and respiratory frequency (**B**, sea bream; **E**, sea bass) in unfed free-swimming fish. At each time point, the mean value of 8 individuals is represented. Mesor is represented by a solid horizontal line, and dashed horizontal lines represent the 20 and 80 percentiles of mean time points. Gray shading represents the dark phase of the light cycle. Arrow marks feeding time (11:00 h) during the pre-recording period. The best-fit curves derived by cosinor analysis are shown as solid lines. Values of mesor (M), amplitude (A) and acrophase (Φ) are stated for each curve. Values represent mean ± SEM (n=8). Asterisks indicate significant differences between species (*P < 0.05, **P < 0.01, ***P < 0.001; Student's t-test), and letters indicate significant differences between both AEFishBIT parameters in a same species (P < 0.05; Student's t-test). **C, F**. Correlation plots for a given time point between physical activity index and respiratory frequency in sea bream (**C**) and sea bass (**F**).

4. Discussion

Traits related to locomotor performance and metabolism are subjected to natural selection as they are often coupled with important behaviors, such as predator evasion, prey capture, reproduction, migration and dominance (Boel et al., 2014; Killen et al., 2014; Seebacher et al., 2013; Walker et al., 2005; Wilson et al., 2013). Moreover, an organism may specialize in one trial at the cost of the other, in which case the trade-off between antagonistic traits evolve causing phenotypic differentiation (Herrel et al., 2009; Heitz, 2014; Walker and Caddigan, 2015; Zhang et al., 2017). In fish, a good example is the trade-off between endurance capacity and sprint speed (Langerhans, 2009; Oufiero et al., 2011), and fish

359 species with “active” lifestyle often have higher rates of dispersal in comparison to
360 sedentary species (Réale et al., 2010; Careau and Garland, 2012). Selection for hypoxia
361 resilience can also co-evolve with faster activity and increased dispersal ratios (Sinclair et
362 al., 2014; Stoffels, 2015), which can be considered a positive trait in wildlife but not in
363 farming conditions where animals cannot escape of deleterious oxygen conditions.
364 Therefore, as reviewed by Davison and Herbert (2013) variations in swimming
365 performance and behavior are of relevance to move towards a more precise and sustainable
366 aquaculture production, although models of fish bioenergetics in swimming metabolic
367 chambers are sometimes not easy to extrapolate to natural or rearing conditions. Indeed,
368 metabolic rates of fish are different when they are moving in linear or non-linear mode
369 (Steinhausen et al., 2010), and interestingly we have observed that jerk accelerations of
370 free-swimming fish at routine speed are apparently higher than those found for forced
371 exercised fish in swim metabolic chambers (Martos-Sitcha et al., 2019). Besides, in-depth
372 analysis of accelerometer records (raw data analysis) also provides valuable information
373 about the amplitude and frequency of the operculum and body tail movements, helping to
374 better phenotype the inter-species differences in locomotor capabilities (see below).

375 Most individual and species variations in locomotor performance and metabolism
376 are coupled and linked to natural evolution as part of the complex behavioral ecology in a
377 predator-prey system (Berger, 2010; Dias et al., 2018). Hence, European sea bass exhibits
378 several morphological and physiological adaptations to sustain its lifestyle as a “fast”
379 swimming predator (Spitz et al., 2013) with a spindle-shaped body that will reduce the
380 water mass moving laterally at each tail stroke. Certainly, hydrodynamic models indicate
381 that, when fish swimming is powered by fast white muscle fibers, muscle contractions are
382 not only faster but possibly of larger amplitude than during slow muscle-powered cruising

(Shadwick et al., 2013; Bale et al., 2015). Thus, comparing exercised European sea bass and gilthead sea bream, we found herein that the amplitude of body tail movements was larger and more stable in European sea bass, without apparent changes at low-medium exercise intensity levels. This might support higher speed accelerations and decelerations as characteristic features of a typical "fast" swimming predator. Indeed, in free-swimming fish, the range of variation of physical activity was also higher in European sea bass, though the average of jerk accelerations on a daily basis was lower in European sea bass than in gilthead sea bream.

Measurements of oxygen consumption are considered good indicators of the energy spent by fish to integrate a wide-range of biological processes, including the stress behavior under different challenging environments (Plaut, 2001; Remen et al., 2016). Thus, direct or indirect measurements of oxygen consumption (e.g. respiratory frequency) are of importance for underlining the metabolic scope of an individual. In this regard, it must be noticed that AEFishBIT calibration in Martos-Sitcha et al. (2019) elicited a close parallelism between measurements of oxygen consumption and respiratory frequency not only during moderate exercise, but also through the anaerobic phase that is largely increased at submaximal exercise (Ejbye-Ernst et al., 2016). As a general statement, we also reported in the first AEFishBIT study that European sea bass exhibits, in comparison to gilthead sea bream, a lower respiration at a given swimming speed, which was viewed as a better adaptation to fast swimming. This assumption was reinforced herein by the observation that a lower frequency of operculum movement was associated with a larger aperture, which in turn was more regulated than the frequency of movement with the increase of swimming speed. All these findings agree with the notion that operculum beats are a reliable measure of metabolic condition and locomotor capabilities in fish having

buccal pumping as a mode of ventilation. However, its relevance is certainly limited in those species (*e.g*. tuna, sharks) that alternate buccal pumping with ram ventilation for covering their high oxygen demand during extreme exercise events (Brill and Brushnell, 2001; Wegner et al., 2010).

It is well known that exercise can profoundly influence the circadian system in rodents (Marchant et al., 1997; Mistlberger et al., 1997; Bobrzynska and Mrosovsky, 1998). In humans, there is also compelling evidence that exercise can elicit significant phase-shifting effects (Van Reeth et al., 1994; Edwards et al., 2002; Buxton et al., 2003) that facilitate the re-entrainment to a shifted light–dark and sleep–wake cycle (Miyazaki et al., 2001; Barger et al, 2004; Yamanaka et al., 2014). Activity patterns are also highly influenced by food availability, and the higher activity of white sea bream (*Diplodus sargus*) during the night in protected areas and artificial reefs is interpreted as the result of a trade-off between predation risk and foraging needs (D'Anna et al., 2011). Early studies in gilthead sea bream also indicate that feeding time (scheduled *vs.* random) affects the behavior and physiology of the animal, and a single daily feeding cycle results beneficial because fish can prepare themselves for the forthcoming feed (Sánchez et al., 2009). Furthermore, in European sea bass and in a lower extent in gilthead sea bream, the percentage of individuals with a diurnal or nocturnal feeding behavior follows a dynamic cycle, which contributes to elicit the dual phasing behavior of some species to cope with anticipatory feed responses and seasonal changes in their environment (Sánchez-Vázquez et al., 1998; Azzaydi et al., 2007; Vera et al., 2013). This also involves daily and seasonal cycles of hormonal activity, synchronized by the light-darkness and feeding-fasting cycles that enable different tissues to act as internal pacemakers (Isorna et al., 2017; Pérez-Sánchez et al., 2018). Certainly, the flexibility of the fish circadian and seasonal system

431 makes these vertebrates a very interesting model for studying the communication between
432 different functional oscillators. However, this relationship is often more complex than
433 initially envisaged, and for instance zebrafish studies revealed an independent phasing
434 between locomotor and feeding activities, which supports the concept of multioscillatory
435 control of circadian rhythmicity in fish (Del Pozo et al., 2011). Thus, in our experimental
436 setup, gilthead sea bream and European sea bass were fed once in the morning (11:00 h)
437 during the pre-recording period, but an anticipatory feed response by measures of physical
438 activity was only especially evident in European sea bass, which might be favored by its
439 lifestyle as a "fast" swimming predator.

440 In any case, the daily cycles of activity and respiration are out of phase in European
441 sea bass, whereas they appeared highly synchronized in gilthead sea bream. This is
442 indicative that swimming is largely fueled by aerobic metabolism in gilthead sea bream, but
443 not in European sea bass that shares in the experimental conditions of the present study a
444 more explosive swimming that would be mostly supported by the anaerobic white muscle
445 fibers. From an energetic point of view, this type of behavior has an important impact on
446 the net energy balance that contributes to explain the bad performance of European sea bass
447 in comparison to gilthead sea bream across the production cycle (Torrecillas et al., 2017;
448 Simó-Mirabet et al., 2018). However, regardless of these different metabolic features,
449 correlation analysis in both European sea bass and gilthead sea bream support that selection
450 for adult body size also selects for enhanced respiration and low activity. In other words,
451 rearing conditions in our experimental facilities prime a phenotypic differentiation between
452 fast growth and low activity and its antagonistic trait (slow growth and high activity) that
453 are highly co-evolved through the evolution of modern teleosts (Rosenfeld et al., 2015;
454 Sibly et al., 2015). From a practical point of view, this indicates that the enhanced energy

cost of growth and maintenance is probably supported by a higher feed intake and perhaps improved feed conversion, as a result of a reduced locomotor activity that does not offer a special advantage in a scenario of intensive production under poorly restricted feeding (Devlin et al., 2004; Killen et al., 2014). Nevertheless, it remains to be established the threshold level of physical activity to assure an active feeding behavior supporting fast growth.

In summary, the present study provides novel insights about the use of AEFishBIT for its use as a reliable tool for remote and individual sensing of fish behavior and metabolic status. It is designed to be attached to the operculum for recording at the same time fish accelerations and respiratory frequency (two in one) as an indicator of intra- and inter-individual fish species differences in the energy portioning between growth and locomotor activities. The achieved results are supported by adaptive changes in body shape and specialized body movements, as a clear evidence that remote and individual monitoring of fish behavior can be used for recognizing beneficial behavioral patterns, which will allow researchers and farmers to select the most convenient lifestyles patterns, to establish stricter criteria of welfare and to improve rearing conditions for a more sustainable and ethical fish production.

Acknowledgements

The authors wish to thank IES *Els Alfacs* (Sant Carles de la Ràpita, Tarragona, Spain) for providing the gilthead sea bream juveniles used in swim respiratory chambers. This project has received funding from the European Union's Horizon 2020 Research and Innovation Programme under grant agreement No. 652831 (AQUAEXCEL^{2020}, Aquaculture

infrastructures for excellence in European fish research towards 2020). This publication reflects the views only of the authors, and the European Commission cannot be held responsible for any use which may be made of the information contained therein. Additional funding was received from National projects: ProID2017010062, from Canarian Agency for Research, Innovation and Information Society (Gobierno de Canarias), co-funded with European Structural and Investment Funds (2014-2020); FICASES, Fish Cage Sensor System (TEC2017-89403-C2-2-R) from Spanish Ministry of Economy, Industry and Competitiveness, co-funded with European Regional Development Funds (2014-2020).

References

Alvarenga, F.A.P., Borges, I., Palkovič, L., Rodina, J., Oddy, V.H., Dobos, R.C, 2016. Using a three-axis accelerometer to identify and classify sheep behaviour at pasture. Appl. Anim. Behav. Sci. 181, 91-99. https://doi.org/10.1016/j.applanim.2016.05.026.

Andrewartha, S.J., Elliott, N.G., McCulloch, J.W. Frappell, P. B., 2016. Aquaculture sentinels: smart-farming with biosensor equipped stock. Journal of Aquaculture Research and Development 7:393. https://doi.org/10.4172/2155-9546.1000393.

Azzaydi, M., Rubio, V.C., López F.J., Sánchez-Vázquez, F.J., Zamora, S., Madrid, J.A., 2007. Effect of restricted feeding schedule on seasonal shifting of daily demand-feeding pattern and food anticipatory activity in European sea bass (*Dicentrarchus Labrax* L.). Chronobiol. Int. 24, 859–74. https://doi.org/10.1080/07420520701658399.

500 Bale, R., Neveln, I.D., Bhalla, A.P.S., MacIver, M.A., Patankar, N.A., 2015. Convergent
501 evolution of mechanically optimal locomotion in aquatic invertebrates and
502 vertebrates. PLoS Biol. 13:e1002123. https://doi.org/10.1371/journal.pbio.1002123.
503 Barger, L.K., Wright, K.P. Jr, Hughes, R.J., Czeisler, C.A., 2004. Daily exercise facilitates
504 phase delays of circadian melatonin rhythm in very dim light. Am. J. Physiol.
505 Regul. Integr. Comp. Physiol. 286, R1077-R1084.
506 https://doi.org/10.1152/ajpregu.00397.2003.
507 Berger, J., 2010. Fear-mediated food webs. In: Terborgh, J., Estes, J.A. (Eds.), Trophic
508 cascades: predators, prey and the changing dynamics of nature. Island Press,
509 Washington, pp. 241-254. https://doi.org/10.1002/wmon.1015.
510 Bobrzynska, K.J., Mrosovsky, N., 1998. Phase shifting by novelty-induced running:
511 activity dose-response curves at different circadian times. J. Comp. Physiol. A. 182,
512 251-258. https://doi.org/10.1007/s003590050175.
513 Boel, M., Aarestrup, K., Baktoft, H., Larsen, T., Søndergaard Madsen, S., Malte, H., Skov,
514 C., Svedsen, J.C., Koed, A., 2014. The physiological basis of the migration
515 continuum in brown trout (*Salmo trutta*). Physiol. Biochem. Zool. 87, 334-345.
516 https://doi.org/10.1086/674869.
517 Brill, R.W., Bushnell, P.G., 2001. The cardiovascular system of tunas. In: Block, B.A.,
518 Stevens, (Eds.), Tuna: Physiology, Ecology, and Evolution. Academic Press, New
519 York, pp. 79-119. https://doi.org/10.1016/S1546-5098(01)19004-7.
520 Brown, D.D., Kays, R., Wikelski, M., Wilson, R., Klimley, A.P., 2013. Observing the
521 unwatchable through acceleration logging of animal behavior. Animal Biotelemetry
522 1:20. https://doi.org/10.1186/2050-3385-1-20.

523 Buxton, O.M., Lee, C.W., L'Hermite-Baleriaux, M., Turek, F.W., Van Cauter, E., 2003.
524 Exercise elicits phase shifts and acute alterations of melatonin that vary with
525 circadian phase. Am. J. Physiol. Regul. Integr. Comp. Physiol. 284, R714-R724.
526 https://doi.org/10.1152/ajpregu.00355.2002.
527 Careau, V., Garland, T., 2012. Performance, personality, and energetics: correlation,
528 causation, and mechanism. Physiological and Biochemical Zoology 18, 3-19.
529 https://doi.org/10.1086/666970.
530 Crouter, S.E., Oody, J.F., Bassett, D.R.Jr., 2018. Estimating physical activity in youth using
531 an ankle accelerometer. Journal of Sports Sciences, 36, 2265-2271.
532 https://doi.org/10.1080/02640414.2018.1449091.
533 D'Anna, G., Giacalone, V.M., Pipitone, C., Badalamenti, F., 2011. Movement pattern of
534 white seabream, *Diplodus sargus* (L., 1758) (Osteichthyes, Sparidae) acoustically
535 tracked in an artificial reef area. Ital. J. Zool. 78, 255–263.
536 https://doi.org/10.1080/11250000903464059
537 Davison, W., Herbert, N.A., 2013. Swimming-enhanced growth. In: Palstra, A.P., Planas,
538 J.V. (Eds.). Swimming Physiology of Fish. Springer-Verlag, Berlin, pp. 177-202.
539 https://doi.org/10.1007/978-3-642-31049-2_8.
540 Del Pozo, A., Sanchez-Ferez, J.A., Sanchez-Vazquez, F.J., 2011. Circadian rhythms of self-
541 feeding and locomotor activity in zebrafish (*Danio rerio*). Chronobiology
542 International 28, 39-47. https://doi.org/10.3109/07420528.2010.530728.
543 De Oliveira, D., Keeling, L.J., 2018. Routine activities and emotion in the life of dairy
544 cows: Integrating body language into an affective state framework. PLoS ONE
545 13:e0195674. https://doi.org/10.1371/journal.pone.0195674.

546 Devlin, R.H., D'Andrade, M., Uh, M., Biagi, C.A., 2004. Population effects of growth
547 hormone transgenic coho salmon depend on food availability and genotype by
548 environment interactions. Proc. Natl. Acad. Sci. USA 101, 9303-9308.
549 https://doi.org/10.1073/pnas.0400023101.
550 Dias, D. M., Campos, C. B., Rodrigues, F. H. G., 2018. Behavioural ecology in a predator-
551 prey system. Mammalian Biology 92, 30-36.
552 https://doi.org/10.1016/j.mambio.2018.04.005.
553 Diaz, M., Fischer, A., Plamondon, R., Ferrer, M.A., 2015. Towards an automatic on-line
554 signature verifier using only one reference per signer. 13th International Conference
555 on Document Analysis and Recognition, 631-635.
556 https://doi.org/10.1109/ICDAR.2015.7333838.
557 Duncan, M. J., Wilson, S., Tallis, J., Eyre, E., 2016. Validation of the Phillips et al.
558 GENEActiv accelerometer wrist cut-points in children aged 5–8 years old. Eur. J.
559 Pediatr. 175, 2019-2021. https://doi.org/10.1007/s00431-016-2795-6.
560 Duval, T., Rémi, C., Plamondon, R., Vaillant, J., O'Reilly, C., 2015. Combining sigma-
561 lognormal modeling and classical features for analyzing graphomotor performances
562 in kindergarten children. Human Movement Science 43, 183-200.
563 https://doi.org/10.1016/j.humov.2015.04.005.
564 Edwards, B., Waterhouse, J., Atkinson, G., Reilly, T., 2002. Exercise does not necessarily
565 influence the phase of the circadian rhythm in temperature in healthy humans. J.
566 Sports Sci. 20, 725-732. https://doi.org/10.1080/026404102320219437.
567 Ejbye-Ernst, R., Michaelsen, T.Y., Tirsgaard, B., Wilson, J.M., Jensen L.F., Steffensen J.
568 F., Pertoldi, C., Aarestrup, K., Svedsen, J.C. 2016. Partitioning the metabolic scope:
569 the importance of anaerobic metabolism and implications for the oxygen- and

570 capacity-limited thermal tolerance (OCLTT) hypothesis. Conserv. Physiol.
571 4:cow019. https://doi.org/10.1093/conphys/cow019.
572 Endo, H., Wu, H., 2019. Biosensors for the assessment of fish health: a review. Fish Sci.
573 85:641. https://doi.org/10.1007/s12562-019-01318-y.
574 Ferrer, M.A., Diaz, M., Carmona, C.A., Plamondon, R., 2018. Idelog: iterative dual spatial
575 and kinematic extraction of sigma-lognormal parameters. IEEE Trans. Pattern Anal.
576 Mach. Intell. https://doi.org/10.1109/TPAMI.2018.2879312.
577 Føre, M., Frank, K., Norton, T., Svendsen, E., Alfredsen, J.A., Dempster, T., Eguiraun, H.,
578 Watson, W., Stahl, A., Sunde, L.M., Schellewald, C., Skøien, K.R., Alver, M.O.,
579 Berckmans, D., 2018. Precision fish farming: a new framework to improve
580 production in aquaculture. Biosyst. Eng. 173, 176-193,
581 https://doi.org/10.1016/j.biosystemseng.2017.10.014.
582 Hamilton, A.W., Davison, C., Tachtatzis, C., Andonovic, I., Michie, C., Ferguson, H.J.,
583 Somerville, L., Jonsson, N.N., 2019. Identification of the rumination in cattle using
584 support vector machines with motion-sensitive bolus sensors. Sensors 19:1165.
585 https://doi.org/10.3390/s19051165.
586 Hassan, W., Føre, M., Ulvund, J.B., Alfredsen, J.A., 2019. Internet of Fish: Integration of
587 acoustic telemetry with LPWAN for efficient real-time monitoring of fish in marine
588 farms. Computers and Electronics in Agriculture 163:104850.
589 https://doi.org/10.1016/j.compag.2019.06.005.
590 Heitz, R.P., 2014. The speed-accuracy trade-off: history, physiology, methodology, and
591 behavior. Front. Neurosci. 8:150. https://doi.org/10.3389/fnins.2014.00150.

592 Herrel, A., Podos, J., Vanhooydonck, B., Hendry, A.P., 2009. Force-velocity trade-off in
593 Darwin's finch jaw function: a biomechanical basis for ecological speciation? Funct.
594 Ecol. 23, 119-125. https://doi.org/10.1111/j.1365-2435.2008.01494.x.

595 Isorna, E., de Pedro, N., Valenciano, A.I., Alonso-Gómez, Á.L., Delgado, M.J., 2017.
596 Interplay between the endocrine and circadian systems in fishes. J. Endocrinol. 232,
597 R141-R159. https://doi.org/10.1530/JOE-16-0330.

598 Jepsen, N., Thorstad, E.B., Havn, T., Lucas, M.C., 2015. The use of external electronic tags
599 on fish: An evaluation of tag retention and tagging effects. Animal Biotelemetry 3,
600 49. https://doi.org/10.1186/s40317-015-0086-z.

601 Killen, S.S., Marras, S, McKenzie, D.J., 2014. Fast growers sprint slower: effects of food
602 deprivation and re-feeding on sprint swimming performance in individual juvenile
603 European sea bass. The Journal of Experimental Biology, 217, 859-865.
604 https://doi.org/10.1242/jeb.097899.

605 Killen, S.S., Mitchell, M.D., Rummer, J.L., Chivers, D.P., Ferrari, M.C.O., Meekan, M.G.,
606 McCormick, M.I., 2014. Aerobic scope predicts dominance during early life in a
607 tropical damselfish. Funct. Ecol. 28, 1367-1376. https://doi.org/10.1111/1365-
608 2435.12296.

609 Langerhans, R.B., 2009. Trade-off between steady and unsteady swimming underlies
610 predator-driven divergence in *Gambusia affins*. Journal of Evolutionary Biology 22,
611 1057-1075. https://doi.org/10.1111/j.1420-9101.2009.01716.x.

612 Marchant, E.G., Watson, N.V., Mistlberger, R.E., 1997. Both neuropeptide Y and serotonin
613 are necessary for entrainment of circadian rhythms in mice by daily treadmill

running schedules. J, Neurosci. 17, 7974-7987. https://doi.org/10.1523/JNEUROSCI.17-20-07974.1997.

Martos-Sitcha, J.A., Sosa, J., Ramos-Valido, D., Bravo, F.J., Carmona-Duarte, C., Gomes, H.L., Calduch-Giner, J.À., Cabruja, E., Vega, A., Ferrer, M.Á., Lozano, M., Montiel-Nelson, J.A., Afonso, J.M., Pérez-Sánchez, J., 2019. Ultra-low power sensor devices for monitoring physical activity and respiratory frequency in farmed fish. Frontiers in Physiology 10:667. https://doi.org/10.3389/fphys.2019.00667.

Michie, C., Andonovic, I., Tachtatzis, C., Davison, C., Konka, J., 2017. Wireless MEMS sensors for precision farming. In: Uttamchandani, D. (Ed.), Wireless MEMS Networks and Applications. Elsevier, Duxford, UK, 2017, pp. 215-238. https://doi.org/10.1016/B978-0-08-100449-4.00010-5.

Mistlberger, R.E., Sinclair, S.V., Marchant, E.G., Neil, L., 1997. Phase-shifts to refeeding in the Syrian hamster mediated by running activity. Physiol. Behav. 61, 273-278. https://doi.org/10.1016/S0031-9384(96)00408-8.

Miyazaki, T., Hashimoto, S., Masubuchi, S., Honma, S., Honma, K.I., 2001. Phase-advance shifts of human circadian pacemaker are accelerated by daytime physical exercise. Am. J. Physiol. Regul. Integr. Comp. Physiol. 281, R197-R237. https://doi.org/10.1152/ajpregu.2001.281.1.R197.

Oufiero, C.E., Walsh, M.R., Reznick, D.N., Garland, T. Jr, 2011. Swimming performance trade-offs across a gradient in community composition in Trinidadian killifish (*Rivulus hartii*). Ecology 92, 170-179. https://doi.org/10.1890/09-1912.1.

Pérez-Sánchez, J., Simó-Mirabet, P., Naya-Català, F., Martos-Sitcha, J.A., Perera, E., Bermejo-Nogales, A., Benedito-Palos, L., Calduch-Giner, J.A., 2018. Somatotropic axis regulation unravels the differential effects of nutritional and environmental

638 factors in growth performance of marine farmed fishes. Frontiers in Endocrinology
639 9:687. https://doi.org/10.3389/fendo.2018.00687.
640 Plamondon, R., O'reilly, C., Galbally, J., Almaksour, A., Anquetil, É., 2014. Recent
641 developments in the study of rapid human movements with the kinematic theory:
642 Applications to handwriting and signature synthesis. Pattern Recognition Letters 35,
643 225-235. https://doi.org/10.1016/j.patrec.2012.06.004.
644 Plaut I., 2001. Critical swimming speed: its ecological relevance. Comp. Biochem. Physiol.
645 A Mol. Integr. Physiol. 131 41–50. https://doi.org/10.1016/S1095-6433(01)00462-
646 7.
647 Pyrkov, T.V., Getmantsev, E., Zhurov, B., Avchaciov, K., Pyatnitskiy, M., Menshikov, L.,
648 Khodova, K., Gudkov, A.V., Fedichev, P.O., 2018. Quantitative characterization of
649 biological age and frailty based on locomotor activity records. Aging 10, 2973-
650 2990. https://doi.org/10.18632/aging.101603.
651 Rajee, O., Alicia, T.K.M., 2019. Biotechnological application in aquaculture and its
652 sustainability constraint. International Journal of Advanced Biotechnology and
653 Research 10, 1-15.
654 Rayas-Amor, A.A., Morales-Almaráz, E., Licona-Velázquez, G., Vieyra-Alberto, R.,
655 García-Martínez, A., Martínez-García, C.G., Cruz-Monterrosa, R.G., Miranda-de la
656 Lama, G.C., 2017. Triaxial accelerometers for recording grazing and ruminating
657 time in dairy cows: An alternative to visual observations. J. Vet. Behav. Clin. Appl.
658 Res. 20, 102–108. https://doi.org/10.1016/j.jveb.2017.04.003.
659 Réale, D., Garant, D., Humphries, M.M., Bergeron, P., Careau, V., Montiglio, P.O., 2010.
660 Personality and the emergence of the pace-of-life syndrome concept at the

661 population level. Philosophical Transactions of the Royal Society B-Biological
662 Sciences, 365, 4051-4063. https://doi.org/10.1098/rstb.2010.0208.
663 Refinetti, R., Cornelissen, G., Halberg, F., 2007. Procedures for numerical analysis of
664 circadian rhythms. Biol. Rhythm. Res. 38, 275-325.
665 https://doi.org/10.1080/09291010600903692.
666 Remen, M., Sievers, M., Torgersen, T., Oppedal, F., 2016. The oxygen threshold for
667 maximal feed intake of Atlantic salmon post-smolts is highly temperature-
668 dependent. Aquaculture 464, 582–592.
669 https://doi.org/10.1016/j.aquaculture.2016.07.037.
670 Roscoe, C.M.P., James, R.S., Duncan, M.J., 2019. Accelerometer-based physical activity
671 levels, fundamental movement skills and weight status in British preschool children
672 from a deprived area. Eur. J. Nucl. Med. Mol. Imaging 178, 1043-1052.
673 https://doi.org/10.1007/s00431-019-03390-z.
674 Rosenfeld, J., Van Leeuwen, T., Richards, J., Allen, D., 2015. Relationship between growth
675 and standard metabolic rate: measurement artefacts and implications for habitat use
676 and life-history adaptation in salmonids. J. Anim. Ecol. 84, 4-20.
677 https://doi.org/10.1111/1365-2656.12260.
678 Rothwell, E.S., Bercovitch, F.B., Andrews, J.R.M., Anderson, M.J., 2011. Estimating daily
679 walking distance of captive African elephants using an accelerometer. Zoo Biology
680 30, 579-591. https://doi.org/10.1002/zoo.20364.
681 Sánchez, J.A., López-Olmeda, J.F., Blanco-Vives, B., Sánchez-Vázquez, F.J., 2009. Effects
682 of feeding schedule on locomotor activity rhythms and stress response in sea bream.
683 Physiol. Behav. 98, 125-129. https://doi.org/10.1016/j.physbeh.2009.04.020.

684 Sánchez-Vázquez, F.J., Azzaydi, M., Martínez, F.J., Zamora, S., Madrid, J.A., 1998.
685 Annual rhythms of demand-feeding activity in sea bass: evidence of a seasonal
686 phase inversion of the diel feeding pattern. Chronobiology International, 15, 607-
687 622. https://doi.org/10.3109/07420529808993197.
688 Seebacher, F., Ward, A.J.W., Wilson, R.S., 2013. Increased aggression during pregnancy
689 comes at a higher metabolic cost. J. Exp. Biol. 216, 771–776.
690 https://doi.org/10.1242/jeb.079756.
691 Shadwick, R.E., Schiller, L.L., Fudge, D.S., 2013. Physiology of swimming and migration
692 in tunas. In: Palstra, A.P., Planas, J.V. (Eds.), Swimming physiology of fish.
693 Springer, Berlin, Germany, pp 45-78. https://doi.org/10.1007/978-3-642-31049-2_3.
694 Sibly, R.M., Baker, J., Grady, J.M., Luna, S.M., Kodric-Brown, A., Venditti, C., Brown,
695 J.H., 2015. Fundamental insights into ontogenetic growth from theory and fish.
696 Proc. Natl Acad. Sci. USA 112, 13934–13939.
697 https://doi.org/10.1073/pnas.1518823112.
698 Simó-Mirabet, P., Perera, E., Calduch-Giner, J.A., Afonso, J.M., Pérez-Sánchez, J., 2018.
699 Co-expression analysis of sirtuins and related metabolic biomarkers in juveniles of
700 gilthead sea bream (*Sparus aurata*) with differences in growth performance.
701 Frontiers in Physiology, 9:608. https://doi.org/10.3389/fphys.2018.00608.
702 Sinclair, E.L.E., De Souza, C.R.N., Ward, A.J.W., Seebacher, F., 2014. Exercise changes
703 behaviour. Functional Ecology 28:652-659. https://doi.org/10.1111/1365-
704 2435.12198.
705 Spitz, J., Chouvelon, T., Cardinaud, M., Kostecki, C., Lorance, P., 2013. Prey preferences
706 of adult sea bass *Dicentrarchus labrax* in the northeastern Atlantic: implications for

bycatch of common dolphin *Delphinus delphis*. ICES J. Mar. Sci. 70, 452-461. https://doi.org/10.1093/icesjms/fss200.

Steinhausen, M.F., Steffensen, J.F., Andersen, N.G., 2010. The effects of swimming pattern on the energy use of gilthead seabream (*Sparus aurata* L.). Mar. Freshw. Behav. Phy. 43, 227-241. https://doi.org/10.1080/10236244.2010.501135.

Stoffels, R.J., 2015. Physiological trade-offs along a fast-slow lifestyle continuum in fishes: what do they tell us about resistance and resilience to hypoxia? PLoS ONE 10:e0130303. https://doi.org/10.1371/journal.pone.0130303.

Thorstad, E.B., Rikardsen, A.H., Alp, A., Økland, F., 2013. The use of electronic tags in fish research—an overview of fish telemetry methods. Turkish J. Fish. Aquat. Sci. 13, 881-896. https://doi.org/10.4194/1303-2712-v13_5_13.

Taylor, L.M., Klenk, J., Maney, A.J., Kerse, N., Macdonald, B.M., Maddison, R., 2014. Validation of a body-worn accelerometer to measure activity patterns in octogenarians. Arch. Phys. Med. Rehabil. 95, 930–934. https://doi.org/10.1016/j.apmr.2014.01.013.

Torrecillas, S., Robaina, L., Caballero, M.J., Montero, D., Calandra, G., Mompel, D., Karalazos, V., Kaushik, S., Izquierdo, M.S., 2017. Combined replacement of fishmeal and fish oil in European sea bass (*Dicentrarchus labrax*): production performance, tissue composition and liver morphology. Aquaculture 474, 101-112. https://doi.org/10.1016/j.aquaculture.2017.03.031.

Vale, S., Trost, S.G., Duncan, M.J., Mota, J., 2015. Step based physical activity guidelines for preschool children. Prev. Med. 70, 78-82. https://doi.org/10.1016/j.ypmed.2014.11.008.

730 Van Reeth, O., Sturis, J., Byrne, M.M., Blackman, J.D., L'Hermite-Balériaux, M., Leproult,
731 R., Oliner, C., Refetoff, S., Turek, F.W., Van Cauter, E. 1994. Nocturnal exercise
732 phase delays circadian rhythms of melatonin and thyrotropin secretion in normal
733 men. Am. J. Physiol. Endocrinol. Metab. 266, E964-E974.
734 https://doi.org/10.1152/ajpendo.1994.266.6.E964.
735 Vera, L.M., Negrini, P., Zagatti, C., Frigato, E., Sánchez-Vázquez, F.J., Bertolucci, C.,
736 2013. Light and feeding entrainment of the molecular circadian clock in a marine
737 teleost (*Sparus aurata*). Chronobiol. Int. 30, 649-661.
738 https://doi.org/10.3109/07420528.2013.775143.
739 Walker, J.A., Ghalambor, C.K., Griset, O.L., McKenney, D., Reznick, D.N., 2005. Do
740 faster starts increase the probability of evading predators? Funct. Ecol. 19, 808-815.
741 https://doi.org/10.1111/j.1365-2435.2005.01033.x.
742 Walker, J.A., Caddigan, S.P., 2015. Performance trade-offs and individual quality in
743 decathletes. Journal of Experimental Biology 218, 3647-3657.
744 https://doi.org/10.1242/jeb.123380.
745 Wegner, N.C., Sepulveda, C.A., Olson, K.R., Hyndman, K.A., Graham, J.B., 2010.
746 Functional morphology of the gills of the shortfin mako, *Isurus oxyrinchus*, a
747 lamnid shark. Journal of Morphology 271, 937-948.
748 https://doi.org/10.1002/jmor.10845.
749 Whitham, J.C., Miller, L.J., 2016. Using technology to monitor and improve zoo animal
750 welfare. Anim. Welf., 25, 395-409. https://doi.org/10.7120/09627286.25.4.395.
751 Wilson, A.M., Lowe, J.C., Roskilly, K., Hudson, P.E., Golabek, K.A., McNutt, J.W., 2013.
752 Locomotion dynamics of hunting in wild cheetahs. Nature 498, 185-192.
753 https://doi.org/10.1038/nature12295.

754 Wilson, R.P., Shepard, E.L.C., Liebsch, N., 2008. Prying into the intimate details of animal
755 lives: use of a daily diary on animals. Endang. Species. Res. 4, 123-137.
756 https://doi.org/10.3354/esr00064.
757 Yamanaka, Y., Hashimoto, S., Masubuchi, S., Natsubori, A., Nishide, S.Y., Honma, S.,
758 Honma, K., 2014. Differential regulation of circadian melatonin rhythm and sleep-
759 wake cycle by bright lights and nonphotic time cues in humans. Am. J. Physiol.
760 Regul. Integr. Comp. Physiol. 307, R546-R557.
761 https://doi.org/10.1152/ajpregu.00087.2014.
762 Zhang, Y.J., Sack, L., Cao, K.F., Wei, X.M., Li, N., 2017. Speed versus endurance tradeoff
763 in plants: Leaves with higher photosynthetic rates show stronger seasonal declines.
764 Scientific Reports 7:42085. https://doi.org/10.1038/srep42085.

765

Supplemental File 1. Accelerometer raw data signal processing.

The opening and closing movement of the operculum was registered by the $a_z(t)$ signal from the tri-axial accelerometer, as it is perpendicular to the operculum. As an illustrative example, two minutes sample of $a_z(t)$ signal is shown in **Figure A.**

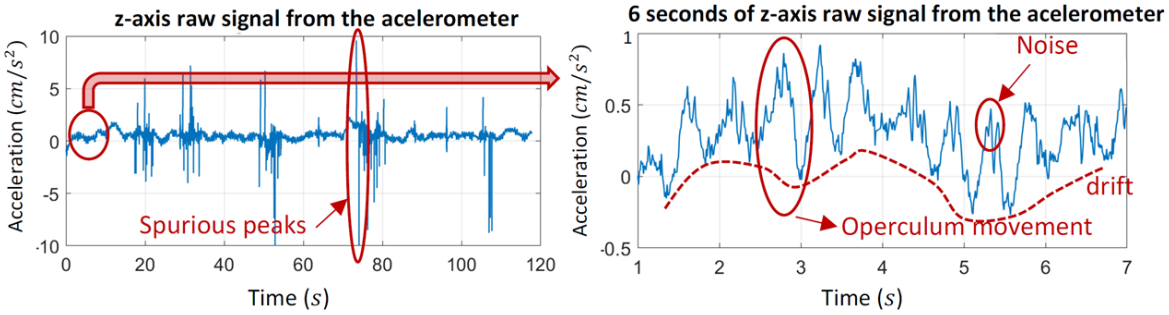

Figure A. Two minutes of raw signal from the z-axis of the accelerometer (left). Zoom out of six seconds of the same signal (right).

In both **Figure A-left** and especially **A-right**, oscillation due to the operculum movement can be observed. **Figure A-left** also shows other contributions to lateral acceleration of the fish in the shape of spurious peaks and superimposed noise added to the sinusoidal-like acceleration waveform. Note that the drift pointed out in **Figure A-left** can be interpreted as an oscillation of the waveform baseline.

Velocity was obtained by integrating the acceleration as:

$$v_{zr}(t) = \int_0^t a_z(t)dt$$

Figure B-left shows an example of the obtained $v_{zr}(t)$. The drift of the accelerometer with non-zero average results in a $v_{zr}(t)$ with a positive slope or trend in the signal which is not real. The operculum movement is oscillating around the trend. To remove this trend and estimate the real velocity of the operculum, the trend of $v_{zr}(t)$ is obtained by low pass filtering of $v_{zr}(t)$ with a cut-off frequency of $f_c = 1\text{Hz}$. This frequency has been selected below the breathing frequency of the fish.

The trend, i.e. the low pass filtered signal of $v_{zr}(t)$, is named $v_{zlp}(t)$. An example of the trend signal $v_{zlp}(t)$ is shown in **Figure B-right**. The difference between $v_{zr}(t)$ (**Figure B-left**) and $v_{zlp}(t)$ (**Figure B-right**) is the superimposed oscillation of $v_{zr}(t)$ around $v_{zlp}(t)$ which is highlighted in **Figure B-center**.

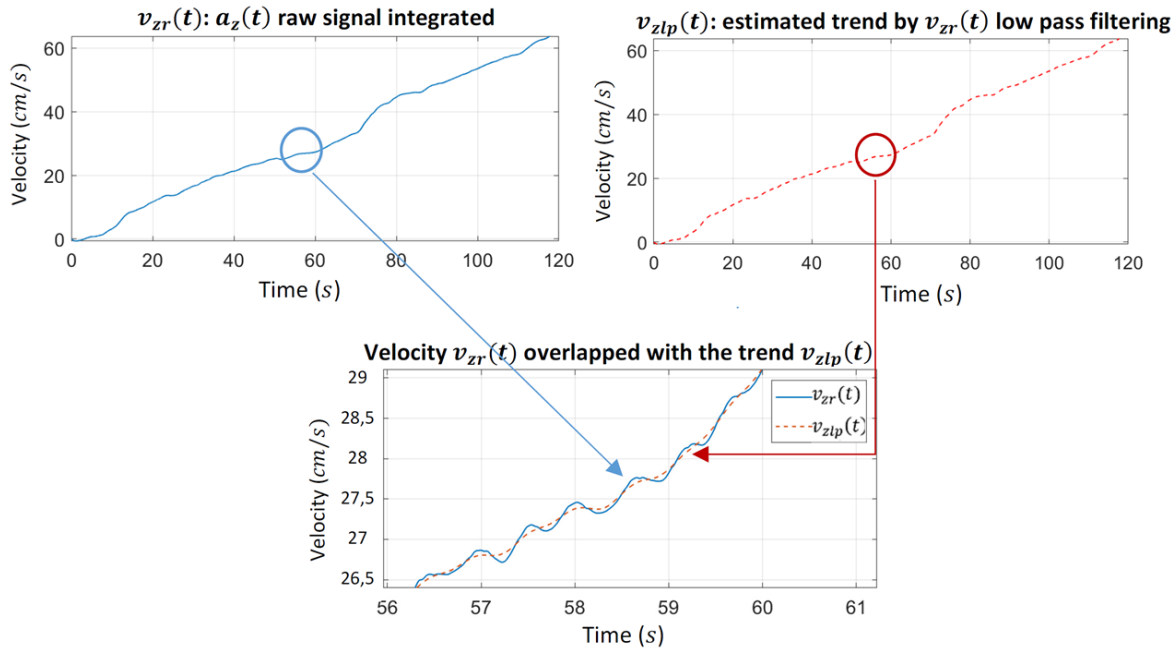

Figure B. $v_{zr}(t)$velocity signal from direct $a_z(t)$ integration (left), trend signal $v_{zlp}(t)$ estimated by low pass filtering of $v_{zr}(t)$ (right). Velocity obtained by straight integration of the acceleration overlapped with the trend. The operculum movement is estimated as the oscillation around the trend (center).

Therefore, the velocity of the operculum is estimated as the detrended signal $v_z(t) = v_{zr}(t) - v_{zlp}(t)$ which is illustrated in **Figure C**. Most of the trend has been removed, but not completely in all the areas of the velocity. This deficiently detrended areas are easily detected as not clear sequence of positive a negative bell-shaped profile of the velocity separated by a zero cross. These areas are removed from the analysis to avoid bias.

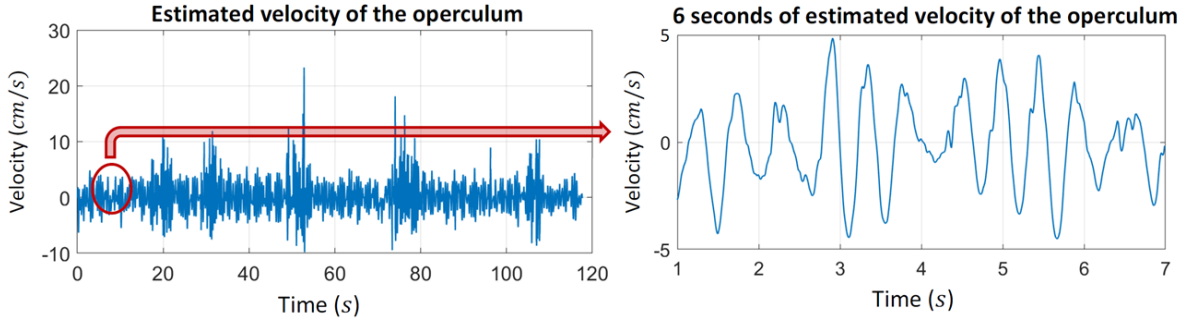

Figure C. Estimated operculum velocity $v_z(t)$ by detrending $v_{zlp}(t)$ (left). Six seconds of the same signal (right).

As the Sigma-Lognormal models the module of the velocity $|v_z(t)|$, **Figure D** shows an example of the module of the estimated velocity.

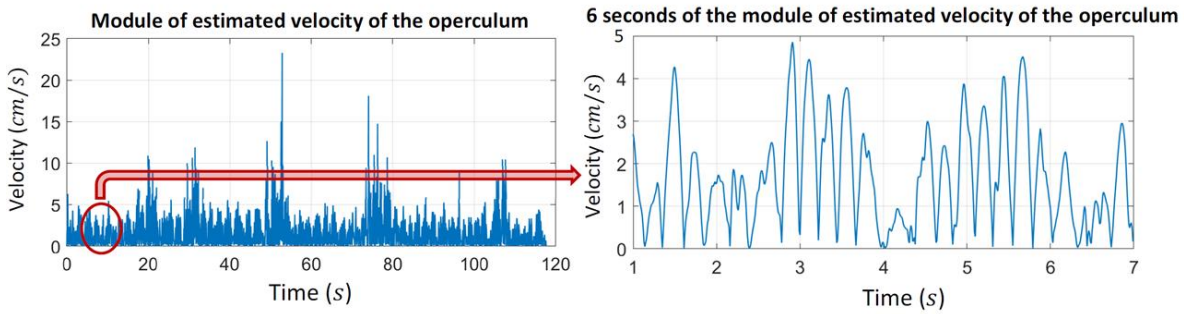

Figure D. Module of the estimated operculum velocity $|v_z(t)|$ (left). Six seconds of the same signal (right)

This same process was carried out with $a_x(t)$ and $a_y(t)$ to obtain $|v_x(t)|$ and $|v_y(t)|$.

Supplemental Figure 1. Comparison of opening and closing operculum movement in gilthead sea bream **(A)** and European sea bass **(B)**.

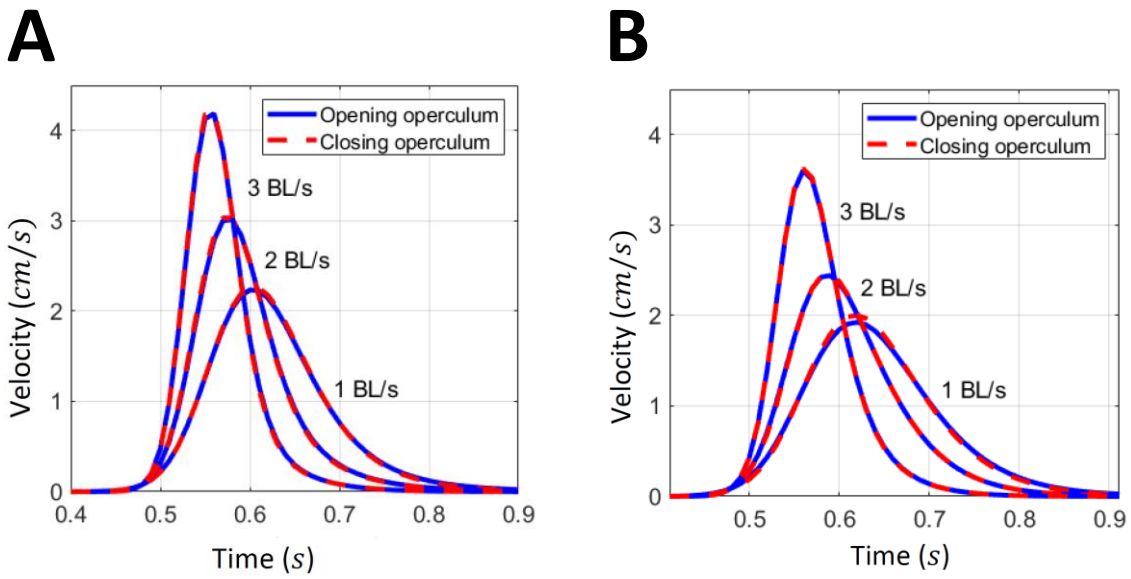

814 **Supplemental Figure 2**. Average values of AEFishBIT records (physical activity index-**A**-
815 , and respiratory frequency-**B**-) in free-swimming gilthead sea bream and European sea
816 bass reared in 3,000 L tanks. Records were calculated for a 2 min time window each 15 min
817 along two complete dark and one complete light phase. Values are mean ± SEM of eight
818 individuals for each fish species. Asterisks represent significant differences ($P < 0.01$) for a
819 given parameter between gilthead sea bream and European sea bass.

820